BPIFB1 loss alters airway mucus properties and diminishes mucociliary clearance

Lauren J. Donoghue[1,2], Matthew R. Markovetz[3], Cameron B. Morrison[3], Kathryn M. McFadden[1], Troy D. Rogers[3], Brian Button[3,4], Camille Ehre[3,5], David B. Hill[3,6], Barbara R. Grubb[3], and Samir N. P. Kelada[1,3]

[1]Department of Genetics, University of North Carolina at Chapel Hill
[2]Curriculum in Genetics and Molecular Biology, University of North Carolina at Chapel Hill
[3]Marsico Lung Institute, University of North Carolina at Chapel Hill
[4]Department of Biochemistry and Biophysics, University of North Carolina at Chapel Hill
[5]Division of Pediatric Pulmonology, University of North Carolina at Chapel Hill
[6]Department of Physics and Astronomy, University of North Carolina at Chapel Hill

ABSTRACT

Airway mucociliary clearance (MCC) is required for host defense and often diminished in chronic lung diseases. Effective clearance depends upon coordinated actions of the airway epithelium and a mobile mucus layer. Dysregulation of the primary secreted airway mucin proteins, MUC5B and MUC5AC, is associated with a reduction in the rate of MCC; however, how other secreted proteins impact the integrity of the mucus layer and MCC remains unclear. We previously identified the gene *Bpifb1* as a regulator of the levels of MUC5B in the airways using genetic approaches. Here, we show that BPIFB1 is required for normal mucociliary clearance *in vivo* using *Bpifb1* knockout (KO) mice. Reduced MCC in *Bpifb1* KO mice occurred in the absence of defects in sodium or chloride ion transport or changes in ciliary beat frequency. We found that BPIFB1 loss resulted in airway mucus flakes with significantly increased complex viscosity, a key biophysical property of mucus known to impact MCC. Finally, BPIFB1 protein colocalized with MUC5B in secretory granules and was present in mucus on the airway surface. Collectively, our findings demonstrate that BPIFB1 is an important component of the mucociliary apparatus in mice and may be a key protein constituent of the mucus network.

INTRODUCTION

The airway mucus layer plays a critical role in airway homeostasis and defense in part by facilitating mucociliary clearance (MCC) of inhaled particles and pathogens. Effective MCC requires a properly hydrated airway surface, an optimal balance of components in secreted mucus (i.e., proteins, salt), and coordinated beating of cilia. The importance of the MCC apparatus is highlighted by the fact that mutations in genes essential to ciliary function or ion transport cause primary ciliary dyskinesia (PCD) and cystic fibrosis (CF), respectively, in which respiratory infections are prominent and severe. In the context of more common obstructive airway disease such as asthma and chronic obstructive pulmonary disease (COPD), changes in MCC have been associated with variation in the abundance of secreted mucin proteins MUC5B and MUC5AC, which are key contributors to the “gel-like” nature of healthy airway mucus[1]. In particular, the concentration, organization, and post-translational modifications of MUC5AC and MUC5B have been shown to alter biophysical properties of mucus that are required for

effective MCC[2–6]. It has also been demonstrated that the ability of mucins to form a proper gel-structure is dependent upon interactions with other secreted proteins, referred to as the "mucin interactome"[7].

In contrast to MUC5AC, which is typically only observed at high levels in disease states, MUC5B is constitutively expressed in the airways of healthy individuals where it has a role in regulating homeostasis through airway MCC and host defense[8,9]. We previously identified the gene *Bpifb1* (also known as *Lplunc1*) as a regulator of airway MUC5B protein levels using a quantitative genetics approach in mice and showed that loss of BPIFB1 (in a knockout mouse model) led to increased levels of MUC5B protein in the airways[10]. Given that MUC5B levels have been shown to affect MCC[9,11], we sought to determine if *Bpifb1* also had a role in regulating MCC. We detected a substantial loss of MCC in the lower airways of *Bpifb1* KO mice. To identify which aspects of the MCC apparatus may be contributing to this defect, we assessed epithelial sodium and chloride ion transport, ciliary function, and biophysical properties of mucus. Our results show that alterations to the mucus layer including increased mucus viscoelasticity were associated with decreased MCC in the absence of BPIFB1*,* while ion transport capacity and ciliary function were maintained.

RESULTS

In order to determine if *Bpifb1* has a role in MCC, we assessed MCC in tracheas of naïve *Bpifb1* KO and WT mice. We quantified MCC by measuring the percentage of instilled beads that were cleared by the trachea over a fixed amount of time. *Bpifb1* KO mice exhibited significantly decreased clearance, with some exhibiting no tracheal bead clearance whatsoever (Fig 1). These results indicate clearly that BPIFB1 is required for MCC.

To understand the mechanism by which BPIFB1 loss leads to defective MCC, we systematically tested the expression and function of key components of the MCC apparatus. First, we examined the expression key ion transporters in the airway epithelium given their importance in regulating airway hydration and MCC[1]. RNA sequencing of lung tissue from *Bpifb1* KO and WT mice did not reveal significant differences in expression of well-characterized sodium and chloride ion transporter genes including *Cftr*, *Scnn1b*, and *Tmem16a* (Fig 2A). However, given that a lack of difference in ion transporter expression does not rule out a difference in functionality, we also measured bioelectric capacities in *Bpifb1* KO and WT tracheas. We found no differences in short-circuit current (I_{sc}) at baseline or following stimulation with compounds targeting the major ion channels in the airway epithelium (i.e. CFTR, ENaC, CaCC), (Fig 2B). This indicated that the loss of MCC in *Bpifb1* KO mice was likely not driven by altered ion transport.

Next, as ciliary beating is essential for MCC, we directly measured ciliary beat frequency (CBF) in intact tracheas *in situ*. In comparison to WT mice, *Bpifb1* KO mice had a slightly elevated CBF, albeit not statistically significant at $P < 0.05$ (Fig 2C). These data indicated that reduced MCC was not associated with a lack of ciliary movement.

To determine if *Bpifb1* loss influenced the expression of other genes or biological processes that could underlie the defect in MCC, we examined global gene expression in lung tissue from *Bpifb1* KO and WT mice. Excluding *Bpifb1*, only 5 protein coding genes and 2 long non-coding RNAs were differentially expressed by genotype (|fold change| $\geq$ 2 and adjusted *P*-value of 0.05, Fig S1). Of these genes, none have been previously annotated for a direct role in MCC or related pathways. Furthermore, genes related to mucin production, including *Muc5b*, *Muc5ac*, *Spdef*, and *Foxa3,* were not differentially expressed. These gene expression results suggested the reduction in MCC in *Bpifb1* KO mice was not mediated by differential expression of key MCC or mucus production genes.

Given the lack of differences in hallmark causes of reduced MCC, we investigated if there were differences in the airway mucus *per se* that could be contributing to the observed loss of MCC. Using microbead rheology, we measured the complex viscosity (η*), a measure of both viscosity and elasticity, of mucus flakes (i.e. the insoluble portions of airway mucus) in bronchoalveolar lavage (BAL) fluid from *Bpifb1* KO vs WT mice. For these measurements, mice were intranasally exposed to house dust mite allergen for three weeks to increase the levels of mucus in BAL, and there were no differences in the degree of eosinophilic inflammation by genotype (Fig S2). We found that the complex viscosity of mucus flakes was significantly increased in *Bpifb1* KO mice compared to WT mice (Fig 3A, B). By imaging of whole BAL, we determined this increase was independent of the size and number of mucus flakes, and there was no difference in these metrics by genotype (Fig S3A-E). Consistent with these findings and our previous report of increased MUC5B in BAL from naïve *Bpifb1* KO mice[10], we found that MUC5B levels were elevated by genotype in the supernatant fraction of centrifuged BAL from naïve mice, but not in the pelleted (i.e. insoluble) fraction (Fig 3C). Thus, loss of BPIFB1 results in increased levels of soluble MUC5B and altered biophysical properties of mucus flakes.

Finally, to gain insight into whether BPIFB1 colocalizes with mucin protein in the airways and, if so, whether this association occurs before mucin granular release, we assessed the spatial relationship between BPIFB1 and mucin protein using fluorescent immunostaining. By colocalization analysis of labeled BPIFB1 and MUC5B protein in large airways of mice challenged with allergen, we determined that the vast majority of MUC5B positive cells were also positive for BPIFB1 (Fig 4A, B), indicating regulated cellular co-expression of MUC5B and BPIFB1. Colocalization was also present in the airways of mice not challenged with allergen (Fig S4). Furthermore, MUC5B positive granules were also positive for BPIFB1 and luminal mucus contained both MUC5B and BPIFB1 (Fig 4C), suggesting that packaging and secretion of these proteins is likely coupled.

Significantly altered levels of either *BPIFB1* gene or protein expression have been observed in CF, COPD, IPF, and asthma[12–15], indicating a strong connection between *BPIFB1* and muco-obstructive diseases. After identifying *Bpifb1* as a regulator of airway mucus levels through an unbiased genome-wide search in the mouse[10], we sought to interrogate the specific function of BPIFB1 in the airways. We found that the loss of BPIFB1 reduced MCC dramatically, demonstrating the critical role of this gene in regulating MCC. Thus, in addition to the strong connection between *BPIFB1* gene or protein expression and muco-obstructive diseases, the fact

that MCC was significantly reduced in naïve *Bpifb1* KO mice indicates BPIFB1 is a regulator of baseline MCC. Studies in humans have shown that there is significant interindividual variation in baseline MCC, and analysis of MCC in monozygotic and dizygotic twins has implicated genetic variation as a modifier of MCC[16]. Given the identification of common genetic variation associated with the levels of *BPIFB1* gene expression[17], it is possible that genetic variation in *BPIFB1* regulation could be one such factor regulating baseline MCC in humans.

DISCUSSION

Due to the lack of differences in basal or stimulated transport of sodium and chloride ions, ciliary beating, and MCC-related gene expression between *Bpfib1* KO and WT mice, our data point toward changes to the airway mucus layer as the cause of reduced MCC. More specifically, the increased complex viscosity of mucus, as we observed in mucus flakes from *Bpifb1* KO mice and may be the case for soluble mucus as well, is suggestive of mucus that is more difficult to clear from the airways. *In vitro* studies with human airway cultures[18–21], as well as earlier studies in model organisms[22–24], have demonstrated that mucus transport is directly related to the rheological properties of mucus. The increased CBF that we observed in *Bpifb1* KO mice, although not statistically significant, may be indicative of an attempt to compensate for altered airways mucus[25]. Such a phenomenon has been demonstrated before, where CBF in human bronchial epithelial cultures increased following a moderate increase in mucus viscosity or mucus load[26].

The increased complex viscosity of mucus flakes that we detected in *Bpifb1* KO mice may be attributable to a change in mucin network structure, which is a function of the density and/or nature of mucin-mucin/mucin-protein interactions[7]. In muco-obstructive airway disease contexts, for example, heightened mucus viscoelasticity due to oxidation-dependent mucin cross-linking[5] or increased mucin concentration[27] has been described. Direct measurement of mucin concentration was not possible in our experiments due to the high dilution factor of mucus in lavage fluid. However, the lack of increased MUC5B in pelleted BAL from *Bpifb1* KO mice provides some evidence against the hypothesis that mucin concentration is increased in mucus flakes and is the driver of changes in mucus rheology. That said, we detected elevated levels of soluble MUC5B in *Bpifb1* KO mice , which raises the question of whether MUC5B levels are higher in *Bpifb1* KO mice simply due to decreased MCC or increased mucin concentration. *In vitro* studies, in which mucus can be collected directly from the surface of epithelial cells, will be required to determine specifically how BPIFB1 impacts the mucus layer.

Although the polymeric nature of gel-forming mucins is essential for the biophysical properties of mucus, studies have shown that mucins alone cannot create complex networks, and thus, other factors, including secreted non-mucin proteins, are necessary for mucus formation[28]. Our results support the conclusion that BPFIB1 is one such protein with an important role in the mucus layer. Further evidence for this determination comes from a finding that in mucus from human bronchial epithelial cells (HEBCs), BPIFB1 has strong physical interactions with mucin proteins. *Radicioni et al*. found that after treating mucus from HBEC cultures with guanidinium hydrochloride and detergents (i.e. dissociative conditions), BPIFB1 was one of few globular

proteins interacting with mucins[7]. Additionally, our data demonstrating shared regulatory mechanisms between BPIFB1 and MUC5B suggest strongly coordinated roles. We previously found that *Bpifb1* and *Muc5b* gene expression was strongly correlated in mouse lung tissue[10], and here we have shown that BPIFB1 and MUC5B protein are colocalized in airway epithelial cells and present in secreted mucus. Cellular co-expression also occurs in human airways on at least the mRNA level, as determined by single cell RNA sequencing studies[29,30]. Lastly, our finding that BPIFB1 is present in mucin secretory granules, which are tightly packed and therefore only contain the necessary proteins for mucus, implicates an additional regulatory mechanism coupling these two proteins. Whether there is an optimal stoichiometry between levels of secreted BPIFB1 and mucin protein for MCC, as may be the case between MUC5B and MUC5AC[2,31], remains to be determined.

In summary, we demonstrate that BPIFB1 is critical for MCC *in vivo*. These findings establish that mucociliary dysfunction can be driven by non-mucin protein components of airway mucus, highlighting their importance in health and disease.

220 **METHODS**

221 *Mice and bronchoalveolar lavage.*

222 *Bpifb1* KO mice were generated as previously described[10]. Female and male homozygous WT
223 and KO littermates were used in all experiments and investigators were blinded to mouse
224 genotype during all data collection. All mice were used at 8-12 weeks and naïve unless
225 otherwise noted. For rheology experiments, mice were intranasally exposed to 25 μg house
226 dust mite allergen (Stallergenes Greer, Cambridge, MA) three times per week for three weeks.
227 Seventy-two hours following the last exposure, bronchoalveolar lavage (BAL) was performed by
228 instilling 500uL of PBS with protease inhibitors into the lungs twice with the same fraction. For
229 differential cell counts on mice under the same allergen protocol, an additional cohort of mice
230 were lavaged with 500uL and 1mL fractions of PBS with protease inhibitors. BAL was spin at
231 500g for 10 min to pellet cells, cells were spun onto slides, and stained with Shandon Kwik Diff
232 Stains(Thermo Scientific). Inflammatory cell counts by two investigators were averaged.
233

234 *Mucociliary clearance.*

235 MCC was measured using a previously described method[32]. Briefly, mice were anesthetized and
236 fluorescent beads were inserted in 200nL PBS through a small incision to approximately the
237 main stem bronchi. After 15 min, tracheas were removed, the tissue was dissolved, and the
238 number of remaining beads were counted.
239

240 *RNA isolation, sequencing, and differential expression analysis.*

241 Lung tissue was harvested from naïve *Bpifb1* WT and KO mice and placed in RNA*later* (Ambion,
242 MilliporeSigma, St. Louis, MO) for 2 weeks. RNA from the right middle lobe was isolated using
243 an RNeasy Kit (Qiagen, Valencia, CA). Sequencing libraries were prepared by the UNC High
244 Throughput Sequencing Facility using the KAPA stranded RNA-seq kit (Roche, Wilmington, MA)
245 and sequenced on a HiSeq4000 (Illumina, San Diego, CA) to a depth of 20 million 50bp single-
246 end reads/sample. Raw reads were evaluated with FastQC
247 (http://www.bioinformatics.babraham.ac.uk/projects/fastqc) and MultiQC[33]. Reads were
248 aligned to the C57BL/6J genome (GENCODE, release M18) using STAR version 2.6.0[34] and
249 quantified with Salmon version 0.9.1[35]. Differential expression was performed using DESeq2
250 version 3.0 with the res() function with contrast KO vs WT[36]. Transcripts with fewer than 10
251 reads in more than 5 samples were excluded from analysis.
252

253 *Ciliary beat frequency.*

254 Ciliary beat frequency (CBF) was measured in situ in the closed trachea, immediately after
255 exsanguination of the mouse anesthetized with 3% isoflurane. For the tracheal preparation, the
256 skin was opened, the muscle and connective tissue overlying the trachea were retracted and
257 the exposed trachea was covered with a piece of plastic wrap dipped in water equilibrated
258 mineral oil. This preparation was immediately placed under a dissecting scope (10x
259 magnification) outfitted with a digital camera (Basler, Germany) and recorded with Basler
260 software. The preparation was lighted a red LED allowing light reflected from the beating cilia
261 to be easily seen. The temperature the preparation was closely monitored using a tiny
262 temperature probe (T Type insect probe, Physitemp Inst. Clifton N. J) placed alongside the
263 trachea. The output from the temperature probe was displayed digitally on a Physitemp TCAT-

2ac Controller and a small ceramic heater (Wuhostam, China) positioned close to the preparation was used to maintain the temperature of the preparation at 37 (± 0.1°C). We found it necessary to place the preparation on an air table (TMC, Peabody MA) to minimize vibrations that interfered with the CBF measurements. It took approximately 3 min from the time of euthanasia until the preparation was under the scope and data acquisition commenced. CBF was measured for a 2 s period at 10, 15, and 20 min after euthanasia. The data were collected at 100 frames/second and analyzed using SAVA software. CBF is reported as the mean of values from the three time points for each mouse. Data from one mouse was excluded because data were missing for two of the three time points.

Ussing chamber bioelectrics.

The bioelectrical proprieties of excised mouse tracheas following euthanasia were obtained using Ussing chambers as previously described [32]. Krebs-Ringer bicarbonate solution was added to the tissue and baseline measurements were taken (Isc), followed by the addition of amiloride (10^{-4} M), forskolin (10^{-5} M), UTP (10^{-4} M), and Bumetanide (10^{-4}M) added sequentially to the basolateral side to block Cl^- secretion.

Histology, immunohistochemistry, and colocalization analysis.

Histological sections were taken from mice sensitized to an immunogenic component of HDM, Der p 1, and challenged with PBS (control) or Der p 1 (allergen challenged) as previously described [10]. Lung tissue was fixed, sectioned, and stained as previously described[10]. Slides were stained with a polyclonal rabbit antibody raised against mouse BPIFB1 (HP8044, Hycult Biotech) at 1:500 and goat polyclonal antibody raised against mouse MUC5B (generously provided by Dr. Alessandra Livraghi-Butrico (UNC)) at 1:1000 for 3 hr at room temperature. Slides without primary antibody or with rabbit IgG (JacksonImmuno) were used as controls. Sections incubated with Alexa Fluor 488 anti-rabbit and Alexa Fluor 594 anti-goat secondaries (Invitrogen) at 1:1000 for 1 hr followed by DAPI at 1:1000 for 5 min. Airway cross-sections cut at the hilum/main stem bronchus were selected for imaging. For each animal, 3-5 representative images of airway epithelium containing goblet cells were taken with an Olympus FV1000 confocal microscope (Olympus, Tokyo, Japan) at 60x magnification using uniform settings. Images were analyzed manually using ImageJ (NIH, Bethesda, Maryland). To determine the number of goblet cells per ROI, the total number of airway epithelial cells and goblet cells were counted and calculated as percentage. To determine colocalization, cells containing MUC5B-positive granules and/or BPIFB1-positive granules were reported as positive for the corresponding marker and calculated as percent of the total number of goblet cells.

Microbead rheology.

Whole/raw BAL samples from allergen exposed mice were mixed with 1-μm carboxylated microspheres. The diffusion of beads through the mixture was tracked and the displacement was estimated using previously described methods[9]. Complex viscosity of the insoluble mucus (flake) fraction of samples was determined using a Gaussian mixture model as described in Esther et al. Samples were excluded from the analysis if their complex viscosity was less than or equal to -2.7, indicating not enough mucus was present in the sample for an accurate measurement.

Whole BAL Imaging.
Whole/raw BAL samples from allergen exposed mice used for microbead rheology measurements were used for imaging. Tiled images were obtained by stitching together sequentially captured viewing fields at 40x in 11 BAL samples per genotype with 3 slides containing 5uL of BAL imaged in each sample. For each field both a fluorescence and a phase contrast image were captured with 10ms exposures in both modalities on an Olympus IX70 inverted light microscope. Images were segmented based on fluorescence intensity into flake and non-flake regions semi-automatically using a MATLAB program (The MathWorks, 2017) and single, user-specified threshold parameter. The threshold that provided the best user-adjudged outline of flake matter, also taking the phase contrast image into account, was used for final determination of flake regions. High-intensity regions of area < 500px (≈25µm in diameter) were excluded as too small to be distinguished from cells or cell debris.

Mucin immunoblotting.
Naïve mice were lavaged with 500uL PBS with protease inhibitors and lavage was spun at 4,000 rpm for 10 min at 4°C. The lavage was then separated into a supernatant fraction and pellet fraction. The pellet fraction was resuspended in 100uL PBS with protease inhibitors. Western blotting for MUC5B was performed as previously described[10,37] with 40uL of supernatant and pellet samples and using a goat polyclonal antibody raised against mouse MUC5B (generously provided by Dr. Alessandra Livraghi-Butrico (UNC)) at 1:500 overnight at 4°C.

Statistics.
Two-sided Student's *t*-tests or Welch's *t*-tests were used to compare values from WT and KO mice for MCC, CBF, and bioelectric assays. Microbead rheology data were log transformed to and analyzed with an ANCOVA model with genotype and experimental batch as covariates. The statistical framework for RNAseq differential expression was performed according to the DESeq2 vignette. All statistical analyses were carried out in R version 3.6.2. Statistical significance was set at a *P* value of 0.05 or less.

Study Approval.
All experiments conducted with mice in this study were compliant with an Institutional Animal Care and Use Committee protocol at an animal facility approved and accredited by the Association for Assessment and Accreditation of Laboratory Animal Care International.

Data availability. Complete raw data and counts generated by RNA sequencing were deposited in the NCBI's Gene Expression Omnibus (GEO) database under entry GSE150452.

AUTHOR CONTRIBUTIONS
LJD, MRM, CBM, BB, CE, DBH, BRG, and SNPK conceived experiments and interpreted data. LJD, MRM, CBM, KMM, and BRG performed experiments. LJD and SNPK wrote and revised the manuscript. All authors edited and reviewed the manuscript.

ACKNOWLEDGEMENTS

We thank Aiman Abzhanova for assistance with immunostaining. This work was supported in part by NIH HL122711 (SNPK). LJD was supported by NIH F31HL143853 and a grant from the National Institute of General Medical Sciences under award 5T32 GM007092.

REFERENCES

1. Fahy J V., Dickey BF. Airway mucus function and dysfunction. *N Engl J Med*. 2011;364(10):978. doi:10.1056/NEJMc1014719
2. Kesimer M, Ford AA, Ceppe A, et al. Airway mucin concentration as a marker of chronic bronchitis. *N Engl J Med*. 2017;377(10):911-922. doi:10.1056/NEJMoa1701632
3. Bonser LR, Zlock L, Finkbeiner W, Erle DJ. Epithelial tethering of MUC5AC-rich mucus impairs mucociliary transport in asthma. *J Clin Invest*. 2016;126(6):2367-2371. doi:10.1172/JCI84910
4. Kesimer M, Makhov AM, Griffith JD, Verdugo P, Sheehan JK. Unpacking a gel-forming mucin : a view of MUC5B organization after granular release. 2018:15-22. doi:10.1152/ajplung.00194.2009.
5. Yuan S, Hollinger M, Lachowicz-Scroggins ME, et al. Oxidation increases mucin polymer cross-links to stiffen airway mucus gels. *Sci Transl Med*. 2015;7(276):1-10. doi:10.1126/scitranslmed.3010525
6. Welsh KG, Rousseau K, Fisher G, et al. MUC5AC and a Glycosylated Variant of MUC5B Alter Mucin Composition in Children With Acute Asthma. *Chest*. 2017;152(4):771-779. doi:10.1016/j.chest.2017.07.001
7. Radicioni G, Cao R, Carpenter J, et al. The innate immune properties of airway mucosal surfaces are regulated by dynamic interactions between mucins and interacting proteins: the mucin interactome. *Mucosal Immunol*. 2016;9(6):1442-1454. doi:10.1038/mi.2016.27
8. Roy MG, Livraghi-Butrico A, Fletcher AA, et al. Muc5b is required for airway defence. *Nature*. 2014;505(7483). doi:10.1038/nature12807
9. Hancock LA, Hennessy CE, Solomon GM, et al. Muc5b overexpression causes mucociliary dysfunction and enhances lung fibrosis in mice. *Nat Commun*. 2018;9(1):1-10. doi:10.1038/s41467-018-07768-9
10. Donoghue L, Livraghi-Butrico A, McFadden K, et al. Identification of trans Protein QTL for Secreted Airway Mucins in Mice and a Causal Role for Bpifb1. *Genetics*. 2017;207(October):801-812. doi:10.1534/genetics.117.300211/-/DC1.1
11. Evans CM, Raclawska DS, Ttofali F, et al. The polymeric mucin Muc5ac is required for allergic airway hyperreactivity. *Nat Commun*. 2015;6(May 2014). doi:10.1038/ncomms7281
12. Bingle L, Wilson K, Musa M, et al. BPIFB1 (LPLUNC1) is upregulated in cystic fibrosis lung disease. *Histochem Cell Biol*. 2012;138(5):749-758. doi:10.1007/s00418-012-0990-8
13. Gao J, Ohlmeier S, Nieminen P, et al. Elevated sputum BPIFB1 levels in smokers with chronic obstructive pulmonary disease: a longitudinal study. *Am J Physiol Lung Cell Mol Physiol*. 2015;309(1):L17-26. doi:10.1152/ajplung.00082.2015
14. Bingle CD, Araujo B, Wallace W a, Hirani N, Bingle L. What is top of the charts?

395 BPIFB1/LPLUNC1 localises to the bronchiolised epithelium in the honeycomb cysts in UIP.
396 *Thorax*. 2013;68(12):1167-1168. doi:10.1136/thoraxjnl-2013-204179
397 15. Wu J, Kobayashi M, Sousa EA, et al. Differential Proteomic Analysis of Bronchoalveolar
398 Lavage Fluid in Asthmatics following Segmental Antigen Challenge. *Mol Cell Proteomics*.
399 2005;4(9):1251-1264. doi:10.1074/mcp.M500041-MCP200
400 16. Camner P, Philipson K, Friberg L. Tracheobronchial Clearance in Twins. 1972:Vol 24.
401 17. Saferali A, Obeidat M, Bérubé J-C, et al. Polymorphisms associated with expression of
402 BPIFA1/BPIFB1 and lung disease severity in cystic fibrosis. *Am J Respir Cell Mol Biol*.
403 2015;53(5):607-614. doi:10.1165/rcmb.2014-0182OC
404 18. King M. Experimental models for studying mucociliary clearance. *Eur Respir J*.
405 1998;11(1):222-228. doi:10.1183/09031936.98.11010222
406 19. Hill DB, Vasquez PA, Mellnik J, et al. A Biophysical Basis for Mucus Solids Concentration
407 as a Candidate Biomarker for Airways Disease. 2014;9(2):1-11.
408 doi:10.1371/journal.pone.0087681
409 20. Button B, Cai LH, Ehre C, et al. A periciliary brush promotes the lung health by separating
410 the mucus layer from airway epithelia. *Science (80-)*. 2012;337(6097):937-941.
411 doi:10.1126/science.1223012
412 21. Carpenter J, Lynch SE, Cribb JA, Kylstra S, Hill DB, Superfine R. Buffer drains and mucus is
413 transported upward in a tilted mucus clearance assay. *Am J Physiol - Lung Cell Mol*
414 *Physiol*. 2018;315(5):L910-L918. doi:10.1152/ajplung.00274.2018
415 22. Shih CK, Litt M, Khan MA, Wolf DP. Effect of nondialyzable solids concentration and
416 viscoelasticity on ciliary transport of tracheal mucus. *Am Rev Respir Dis*. 1977;115(6):989-
417 995. doi:10.1164/arrd.1977.115.6.989
418 23. Lorenzi G, Bohm GM, Guimaraes ET, Costa Vaz MA, King M, Saldiva PHN. Correlation
419 between rheologic properties and in vitro ciliary transport of rat nasal mucus.
420 *Biorheology*. 1992;29(4):433-440. doi:10.3233/BIR-1992-29406
421 24. Yu DM, Amidon GL, Weiner ND, Fleisher D, Goldberg AH. The Role of Rheological
422 Properties in Mucociliary Transport by Frog Palate Ciliated Model. *Pharm Res*.
423 1994;11(12).
424 25. Button B, Okada SF, Frederick CB, Thelin WR, Boucher RC. Mechanosensitive ATP release
425 maintains proper mucus hydration of airways. *Sci Signal*. 2013;6(279):1-10.
426 doi:10.1126/scisignal.2003755
427 26. Liu L, Shastry S, Byan-Parker S, et al. An autoregulatory mechanism governing mucociliary
428 transport is sensitive to mucus load. *Am J Respir Cell Mol Biol*. 2014;51(4):485-493.
429 doi:10.1165/rcmb.2013-0499MA
430 27. Esther CR, Muhlebach MS, Ehre C, et al. Mucus accumulation in the lungs precedes
431 structural changes and infection in children with cystic fibrosis. *Sci Transl Med*.
432 2019;11(486). doi:10.1126/scitranslmed.aav3488
433 28. Thornton DJ, Sheehan JK. From mucins to mucus: toward a more coherent understanding
434 of this essential barrier. *Proc Am Thorac Soc*. 2004;1(1):54-61. doi:10.1513/pats.2306016
435 29. Braga FAV, Kar G, Berg M, et al. Cell States in Health and in Asthma. *Nat Med*. 2019.
436 30. Goldfarbmuren KC, Jackson ND, Sajuthi SP, et al. Dissecting the cellular specificity of
437 smoking effects and reconstructing lineages in the human airway epithelium. *bioRxiv*.
438 2019:612747. doi:10.1101/612747

439 31. Kirkham S, Kolsum U, Rousseau K, Singh D, Vestbo J, Thornton DJ. MUC5B is the major
440 mucin in the gel phase of sputum in chronic obstructive pulmonary disease. *Am J Respir*
441 *Crit Care Med*. 2008;178(10):1033-1039. doi:10.1164/rccm.200803-391OC
442 32. Grubb BR, Livraghi-Butrico A, Rogers TD, Yin W, Button B, Ostrowski LE. Reduced
443 mucociliary clearance in old mice is associated with a decrease in Muc5b mucin. *Am J*
444 *Physiol - Lung Cell Mol Physiol*. 2016;310(9):L860-L867. doi:10.1152/ajplung.00015.2016
445 33. Ewels P, Magnusson M, Lundin S, Käller M. MultiQC: Summarize analysis results for
446 multiple tools and samples in a single report. *Bioinformatics*. 2016;32(19):3047-3048.
447 doi:10.1093/bioinformatics/btw354
448 34. Dobin A, Davis CA, Schlesinger F, et al. STAR: Ultrafast universal RNA-seq aligner.
449 *Bioinformatics*. 2013;29(1):15-21. doi:10.1093/bioinformatics/bts635
450 35. Patro R, Duggal G, Love MI, Irizarry RA, Kingsford C, Biology C. Salmon: fast and bias-
451 aware quantification of transcript expression using dual-phase inference. *Nat Methods*.
452 2017;14(4):417-419. doi:10.1038/nmeth.4197.Salmon
453 36. Love MI, Huber W, Anders S. Moderated estimation of fold change and dispersion for
454 RNA-seq data with DESeq2. *Genome Biol*. 2014;15(12):550. doi:10.1186/s13059-014-
455 0550-8
456 37. Ramsey KA, Rushton ZL, Ehre C. Mucin agarose gel electrophoresis: Western blotting for
457 high-molecularweight glycoproteins. *J Vis Exp*. 2016;2016(112):2-7. doi:10.3791/54153
458

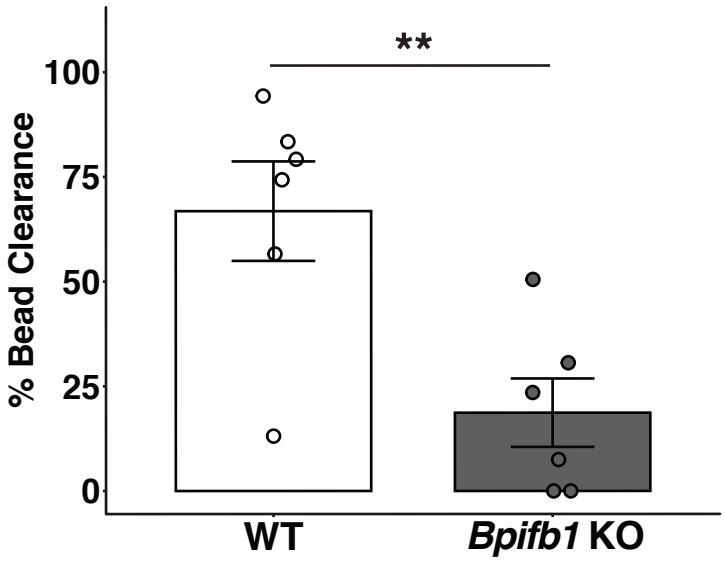

Figure 1. Decreased mucociliary clearance in *Bpifb1* KO mice. Percent bead clearance in tracheal mucociliary clearance assay in naive WT and *Bpifb1* KO mice. Mean ± SEM depicted. n=6/genotype. Significance of two-sided Student's *t*-test denoted as **, $P < 0.01$.

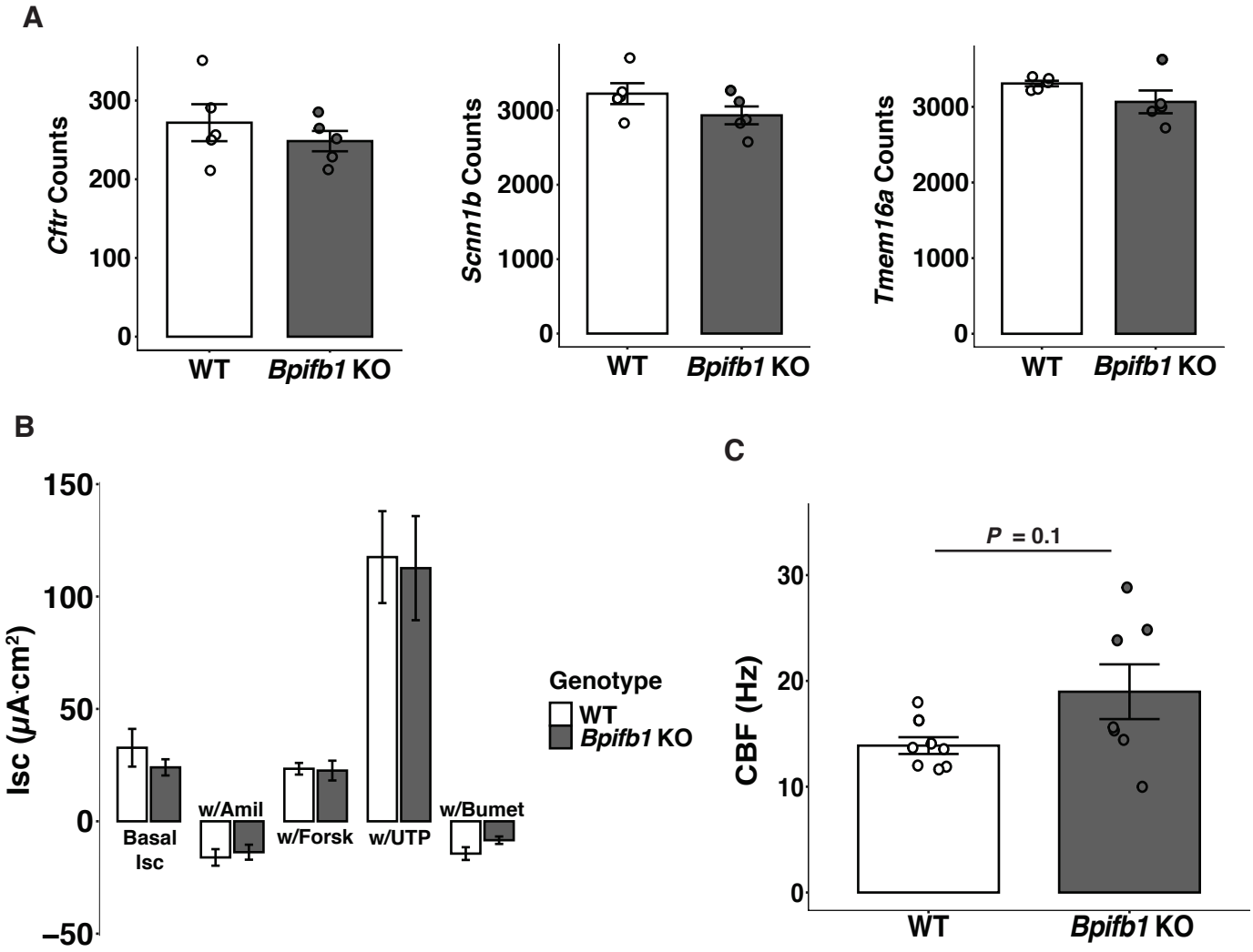

Figure 2. Ion transport and ciliary beat are not different in *Bpifb1* KO mice.
(A) No genotype difference in gene expression of ion channel genes *Cftr*, *Scnn1b*, and *Tmem16a*. (B) Ion transport measured in Ussing chambers. Mean ± SEM depicted. n=6/genotype. No differences between genotypes by two-sided Student's *t*-test. (C) Ciliary beat frequency in tracheal ring assay. Mean ± SEM depicted. n=7-8/genotype. Difference between genotypes not significant by two-sided Welch's *t*-test, $P = 0.1$.

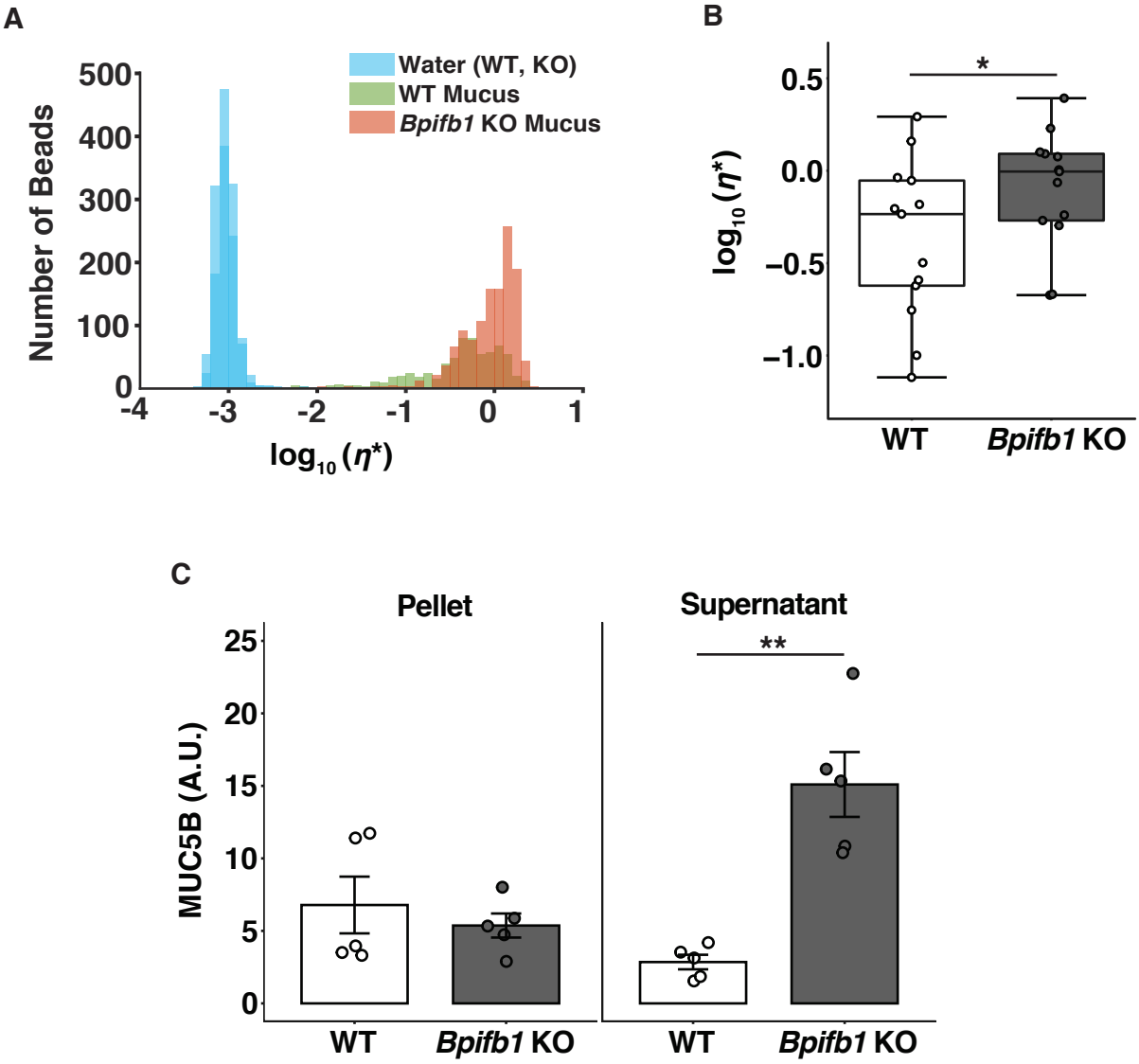

Figure 3. Biophysical properties of airway mucus are altered in *Bpifb1* KO mice. (A) Distribution of rheological signal in BAL from a representative allergen exposed WT and *Bpifb1* KO mouse. (B) Complex viscosity of BAL mucus fraction. Boxplots depict median and interquartile ranges. n=13/genotype. Significant difference between genotypes by ANOVA modeling denoted as *, $P < 0.05$. (C) MUC5B in pellet and supernatant fractions of BAL from naive WT and *Bpifb1* KO mice by mucin western blotting. Mean ± SEM depicted. Significant difference between genotypes for supernatant fraction by two-sided Welch's *t*-test denoted as **, $P < 0.01$. n=5/genotype.

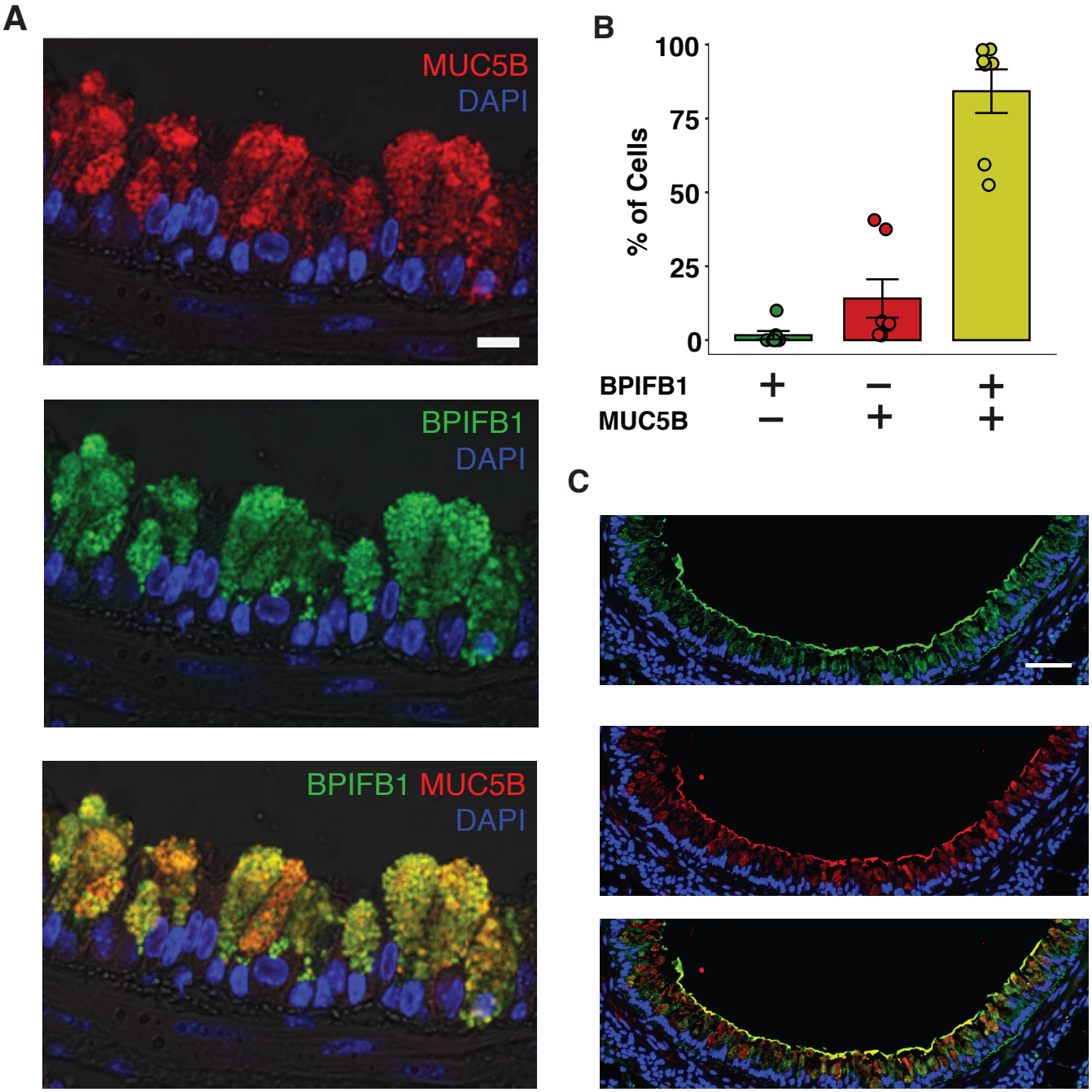

Figure 4: BPIFB1 and MUC5B colocalize in airway epithelial cells. (A) BPIFB1 (green) and MUC5B (red) immunostaining in airway epithelial cells from allergen challegned mice. Scale bar = 10 μm. (B) Percentage of cells positively stained for BPIFB1 only, MUC5B only, or both in allergen challenged mice. (C) BPIFB1 (green) and MUC5B (red) immunostaining in large airways of allergen challegned mice demonstrating BPIFB1 staining in luminal mucus. Scale bar = 50 μm.